

Local study of a renormalization operator for 1D maps under quasiperiodic forcing*

Àngel Jorba¹, Pau Rabassa² and Joan Carles Tatjer¹

September 22nd, 2015

¹ Departament de Matemàtica Aplicada i Anàlisi, Universitat de Barcelona, Gran Via 585, 08007 Barcelona, Spain

² School of Mathematical Sciences, Queen Mary University of London, Mile End Road, London E1 4NS, United Kingdom

Abstract

The authors have recently introduced an extension of the classical one dimensional (doubling) renormalization operator to the case where the one dimensional map is forced quasiperiodically. In the classic case the dynamics around the fixed point of the operator is key for understanding the bifurcations of one parameter families of one dimensional unimodal maps. Here we perform a similar study of the (linearised) dynamics around the fixed point for further application to quasiperiodically forced unimodal maps.

1 Introduction

Given a one-dimensional dynamical system, one can consider a quasiperiodic forcing of its dynamics, given place to *quasiperiodically forced one dimensional map* of the form

$$F : \mathbb{T} \times \mathbb{R} \rightarrow \mathbb{T} \times \mathbb{R} \\ \begin{pmatrix} \theta \\ x \end{pmatrix} \mapsto \begin{pmatrix} \theta + \omega \\ f(\theta, x) \end{pmatrix}$$

where $\mathbb{T} = \mathbb{R}/\mathbb{Z}$, $f \in C^r(\mathbb{T} \times \mathbb{R}, \mathbb{R})$ with $r \geq 1$ and $\omega \in \mathbb{T} \setminus \mathbb{Q}$. In other words, a skew map where the dynamics on one of its component is given by a solid rotation of angle ω . Therefore, a map of this form can be identified with a pair (ω, f) with ω and f as before.

We are interested in quasiperiodic forced maps as perturbations of one dimensional maps [15, 4, 5, 6, 9, 8]. The paradigmatic example is a two parametric map $f(\theta, x) = f(\theta, x, \alpha, \varepsilon)$ with

$$f(\theta, x, \alpha, \varepsilon) = g(x, \alpha) + \varepsilon h(\theta, x, \alpha, \varepsilon),$$

*Work supported by the MEC grant MTM2012-32541 and the AGAUR grant 2014 SGR 1145.

where g and h are C^∞ functions. Typically, it is assumed that the one-parameter family $g(\cdot, \alpha)$ has a cascade of period doubling bifurcations. Between each of these bifurcations, a superstable periodic orbit is known to exist. An example of such a family is the well-known Logistic Map $g(x, \alpha) = \alpha x(1 - x)$.

In [16] we showed the existence of some universality and self-renormalization properties in the parameter space of the Forced Logistic Map, although the phenomena of universality and self-renormalization are a bit different with respect to the one-dimensional case. Concretely, the rotation number is shown to have a crucial role. In [7] we introduced an extension of the classical one dimensional (doubling) renormalization operator to cover the quasiperiodic forcing of the map. In the classic operator the dynamics around the fixed point of the operator plays a crucial role to understand the bifurcations of one-parametric families of one dimensional unimodal maps [2]. Here we perform an equivalent study of the (linearised) dynamics around the fixed point for further application to quasiperiodically forced unimodal maps.

In the remainder of this section we review the extension of the operator introduced in [16]. In Section 2 we study, both analytically and numerically, the properties of the linearized operator. Section 3 is devoted to a numerical study of the dynamics of the linearised operator. If the dynamics is projected on the unit sphere (of the corresponding function space) it seems that there exists an attractor that looks like a dyadic solenoid. A detailed study is actually work in progress.

1.1 A setup for the 1D renormalization operator

Let us review the definition of the 1D renormalization operator in a set up that is suitable for introducing a quasiperiodic perturbation to the 1D map.

Given a small value $\delta \geq 0$, let \mathcal{M}_δ denote the space of C^r ($r \geq 1$) even maps ψ of the interval $I_\delta = [-1 - \delta, 1 + \delta]$ into itself such that

M1. $\psi(0) = 1$,

M2. $x\psi'(x) < 0$ for $x \neq 0$.

Set $a = \psi(1)$, $a' = (1 + \delta)a$ and $b' = \psi(a')$. We define $\mathcal{D}(\mathcal{R}_\delta)$ as the set of $\psi \in \mathcal{M}_\delta$ such that

D1. $a < 0$,

D2. $1 > b' > -a'$,

D3. $\psi(b') < -a'$.

Conditions M1 and M2 require the map to be unimodal with 0 as the critical point. Conditions D1, D2 and D3 ensure that the intervals $[-a', a']$ and $[b', 1]$ do not overlap and each one is mapped into the other. In Figure 1.1 we include a schematic plot of a map in \mathcal{M}_δ where the geometric meaning of the values a , a' and b' is shown.

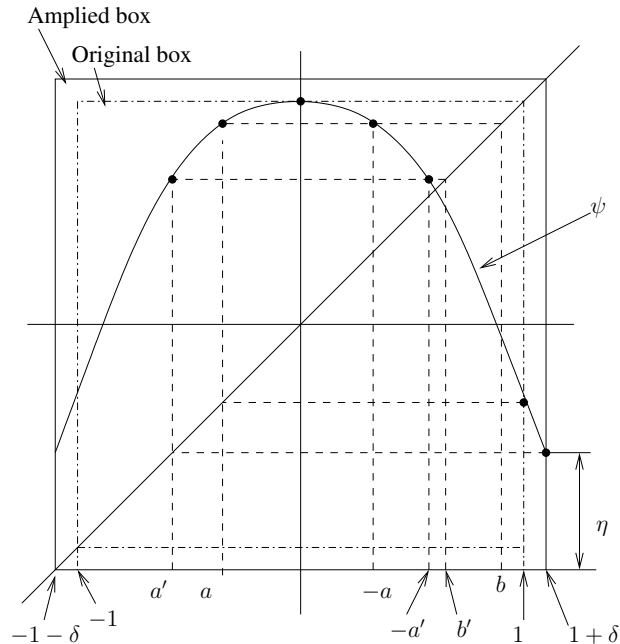


Figure 1: Schematic plot of a map in \mathcal{M}_δ . The geometric meaning of the values a , a' , b' , δ and η are shown.

We define the (1D doubling) *renormalization operator* $\mathcal{R}_\delta : \mathcal{D}(\mathcal{R}_\delta) \rightarrow \mathcal{M}_\delta$ as

$$\mathcal{R}_\delta(\psi)(x) = \frac{1}{a} \psi \circ \psi(ax).$$

with $a = \psi(1)$. Let $\mathcal{D}^n(\mathcal{R}_\delta)$ denote the set of functions which are n times renormalizable:

$$\mathcal{D}^n(\mathcal{R}_\delta) = \{f_0 \in \mathcal{M}_\delta \mid f_i = \mathcal{R}_\delta^i(f_0) \in \mathcal{D}(\mathcal{R}_\delta), \text{ for } i = 0, \dots, n-1, \}$$

The setup for the renormalization operator given above is a small modification of the one introduced in [12], which is recovered for $\delta = 0$. The modification done here is to ensure that one dimensional maps can be quasiperiodically perturbed further on and remain well defined. In [7] it is shown that the operator \mathcal{R}_δ is well defined, and that any fixed point of \mathcal{R}_0 extends to a fixed point of \mathcal{R}_δ for δ small enough.

1.2 The quasiperiodically forced case

Consider a quasiperiodically forced map, with its domain restricted to the compact cylinder $\mathbb{T} \times I_\delta$:

$$F : \mathbb{T} \times I_\delta \rightarrow \mathbb{T} \times I_\delta$$

$$\begin{pmatrix} \theta \\ x \end{pmatrix} \mapsto \begin{pmatrix} \theta + \omega \\ f(\theta, x) \end{pmatrix}, \quad (1)$$

with ω an irrational number, f a C^r function and $I_\delta = [-(1 + \delta), 1 + \delta]$. Given $F = (\omega, f)$ a quasiperiodically forced map, its renormalization $R(F)$ is defined as an affine transformation applied to $F^2 = F \circ F$ (the self-composition of F). The map F^2 is of the form $(2\omega, f^2)$, with $f^2(\theta, x) = f(\theta + \omega, f(\theta, x))$. The extension of the renormalization operator proposed in [7] is of the form $R(F) = (2\omega, \mathcal{T}_\omega(f))$, with $\mathcal{T}_\omega(f)$ an affine transformation of f^2 . In other words, the affine transformation applied to F^2 is just a multiplication by two in the ω -component. With this definition we obtain an operator that preserves the skew structure of the maps.

We introduce now some notation for the definition of $\mathcal{T}_\omega(f)$. Let us identify $C^r(I_\delta, I_\delta)$ with its natural inclusion in $C^r(\mathbb{T} \times I_\delta, I_\delta)$ defined as $[i(f)](\theta, x) = f(x)$ for any $f \in C^r(I_\delta, I_\delta)$. With this identification $C^r(I_\delta, I_\delta)$ is a subspace of $C^r(\mathbb{T} \times I_\delta, I_\delta)$ and the operator

$$\begin{aligned} p_0 : C^r(\mathbb{T} \times I_\delta, I_\delta) &\rightarrow C^r(I_\delta, I_\delta) \\ f &\mapsto \int_0^1 f(\theta, x) d\theta, \end{aligned}$$

defines a projection. Then, we can consider \mathcal{M}_δ and $\mathcal{D}(\mathcal{R}_\delta)$ as sets in both $C^r(I_\delta, I_\delta)$ and $C^r(\mathbb{T} \times I_\delta, I_\delta)$ depending on the context. Consider also \mathcal{X}_δ , the set defined as

$$\mathcal{X}_\delta = \{f \in C^r(\mathbb{T} \times I_\delta, I_\delta) \mid p_0(f) \in \mathcal{M}_\delta\}.$$

Given a function $g \in \mathcal{X}_\delta$, we define the (*quasiperiodic doubling*) *renormalization* of g as

$$[\mathcal{T}_\omega(g)](\theta, x) := \frac{1}{\hat{a}} g(\theta + \omega, g(\theta, \hat{a}x)), \quad (2)$$

where $\hat{a} = \int_0^1 g(\theta, 1) d\theta$.

The operator \mathcal{T}_ω restricted to the set $\mathcal{D}(\mathcal{R}_\delta)$ coincides with the operator \mathcal{R}_δ . Therefore, any fixed point of \mathcal{R}_δ extends to a fixed point of \mathcal{T}_ω . Consider the set $\mathcal{D}(\mathcal{T}_\omega) = \{g \in \mathcal{X}_\delta \mid \mathcal{T}_\omega(g) \in \mathcal{X}_\delta\}$, then the renormalization operator \mathcal{T}_ω is defined from $\mathcal{D}(\mathcal{T}_\omega)$ to \mathcal{X}_δ . Actually, $\mathcal{D}(\mathcal{T}_\omega)$ contains an open neighbourhood (in \mathcal{X}_δ) of $\mathcal{D}(\mathcal{R}_\delta)$, where the operator is well defined [7].

At this point we can go back to the definition of R , the renormalization operator for a quasiperiodically forced map $F = (\omega, f)$ like (1).

Consider

$$\begin{aligned} X &= \{(\omega, f) \in \mathbb{T} \times C^r(\mathbb{T} \times I_\delta, I_\delta) \mid f \in \mathcal{X}_\delta\}, \\ \mathcal{D}(R) &= \{(\omega, f) \in \mathbb{T} \times C^r(\mathbb{T} \times I_\delta, I_\delta) \mid f \in \mathcal{D}(\mathcal{T}_\omega)\}. \end{aligned}$$

We define the *quasiperiodically forced renormalization operator* as

$$\begin{aligned} R : \mathcal{D}(R) &\rightarrow X \\ (\omega, f) &\mapsto (2\omega, \mathcal{T}_\omega(f)). \end{aligned}$$

Let $\mathcal{D}^n(R)$ denote the domain of maps (ω, f) which are n -times renormalizable, in other words

$$\mathcal{D}^n(R) = \left\{ (\omega_0, f_0) \in X \mid \begin{array}{l} f_i \in \mathcal{D}(\mathcal{T}_{\omega_i}), \text{ for } i = 0, \dots, n-1, \\ \text{where } (\omega_i, f_i) := R(\omega_{i-1}, f_{i-1}) \end{array} \right\}.$$

Consider Φ the Feigenbaum fixed point of \mathcal{R}_δ given by [12]. Then Φ is also fixed by \mathcal{T}_ω and the set $\mathbb{T} \times \{\Phi\}$ is invariant by R and the dynamics in ω is determined by the expansive map $\omega_{n+1} = 2\omega_n$.

1.3 Differentiability of the operator and its tangent map

Given $\phi \in \mathcal{D}(\mathcal{T}_\omega)$, $\phi \in C^{r+s}$, there exists an open neighbourhood U of ϕ in $\mathcal{D}(\mathcal{T}_\omega)$ in the C^{r+s} topology, such that $\mathcal{T}_\omega : U \rightarrow \mathcal{X}_\delta$ with the C^r topology is a C^s operator [7]. This gives place to an obvious ‘‘loss of differentiability’’. An alternative to fix this problem is to consider a setup of the operator on the analytic functions.

Let B_ρ be a complex band of width ρ around the real numbers ($B_\rho = \{z = x + iy \in \mathbb{C} \text{ such that } |y| < \rho\}$) and W be an open, bounded and simply connected set in \mathbb{C} containing the real interval I_δ . Consider $\mathcal{B}(B_\rho, W)$ the space of functions $f : B_\rho \times W \rightarrow \mathbb{C}$ such that:

1. f is holomorphic in $B_\rho \times W$ and continuous in the closure of $B_\rho \times W$.
2. f is real analytic (it maps real numbers to real numbers).
3. f is 1-periodic in the first variable, i. e. $f(\theta+1, z) = f(\theta, z)$ for any $(\theta, z) \in B_\rho \times W$.

The space $\mathcal{B}(B_\rho, W)$ endowed with the supremum norm is a Banach space.

Let us define $\mathcal{B}(W)$ as the space of real analytic functions that are holomorphic in W and continuous in its closure, equipped with the supremum norm. This is the one dimensional counterpart of $\mathcal{B}(B_\rho, W)$, and we can understand $\mathcal{B}(W)$ as a subset of $\mathcal{B}(B_\rho, W)$.

We want to consider the operator \mathcal{T}_ω in the new topology of $\mathcal{B}(B_\rho, W)$. Given $f \in \mathcal{B}(B_\rho, W)$, a necessary condition to have $\mathcal{T}_\omega(f)$ well defined is that $f(B_\rho \times \hat{a}(f)W) \subset W$ (where $aW = \bigcup_{z \in W} \{az\}$). In [12] it is shown that there exist a set W and a function Φ such that $\Phi \in \mathcal{D}(\mathcal{R}_0) \cap \mathcal{B}(W)$ and Φ is a fixed point of \mathcal{R}_0 (hence a fixed point of \mathcal{T}_ω as well). In [7] it is shown that, for a sufficiently small ρ , there exists $U \subset \mathcal{B}(B_\rho, W)$, an open neighbourhood of Φ , such that $\mathcal{T}_\omega(\Psi)$ is well defined for any $\Psi \in U$. It is also shown that \mathcal{T}_ω is Fréchet differentiable for any $\Psi \in U$ and its derivative is equal to

$$\begin{aligned} [D\mathcal{T}_\omega(\Psi)h](\theta, x) &= \frac{1}{a}(\partial_x \Psi)(\theta + \omega, \Psi(\theta, ax))h(\theta, ax) + \frac{1}{a}h(\theta + \omega, \Psi(\theta, ax)) \\ &\quad + \frac{b}{a}(\partial_x \Psi)(\theta + \omega, \Psi(\theta, ax))(\partial_x \Psi(\theta, ax))x - \frac{b}{a^2}\Psi(\theta + \omega, \Psi(\theta, ax)), \end{aligned}$$

with $a = \int_0^1 \Psi(\theta, 1)d\theta$ and $b = \int_0^1 h(\theta, 1)d\theta$.

One of the reasons to introduce the (quasiperiodically forced) renormalization operator is to study the image by R of functions of the form $F = (\omega_0, f_0) + \varepsilon(0, h_0)$ where ω_0 is a Diophantine number, $f_0 \in \mathcal{D}(\mathcal{R}_\delta)$, ε is a small parameter and $h_0 \in T_{\omega_0, f_0}X$. In other words, we are interested only in (infinitesimal) perturbations $\delta F \in T_F X$ that preserve the skew product structure of maps like (1). For this reason we will only consider tangent vectors of the form $\delta F = (0, \delta f)$. We can incorporate this in the tangent bundle of X and (re)define it as:

$$TX = \{(\omega, f, h) \mid (\omega, f) \in X, \quad (0, h) \in T_{(\omega, f)}X\}.$$

We can define now S , the *tangent map associated to R* , in the C^r topology as

$$\begin{aligned} S : \mathcal{D}(S) &\rightarrow TX \\ (\omega, f, h) &\mapsto (2\omega, \mathcal{T}_\omega(f), D\mathcal{T}_\omega(f)h), \end{aligned} \quad (3)$$

with $\mathcal{D}(S) := \{(\omega, f, h) \in TX \mid (\omega, f) \in \mathcal{D}(R) \text{ and } f \in C^{r+1}(\mathbb{T} \times I_\delta, I_\delta)\}$.

2 Properties of $D\mathcal{T}_\omega$

2.1 Fourier expansion of $D\mathcal{T}_\omega$

Let Ψ be a function in a neighbourhood of Φ (the fixed point of \mathcal{T}_ω) where the operator \mathcal{T}_ω is differentiable. Additionally, assume that $\Psi \in \mathcal{D}(\mathcal{T}_\omega)$.

Given a function $f \in \mathcal{B}(B_\rho, W)$ we can consider its complex Fourier expansion in the periodic variable

$$f(\theta, z) = \sum_{k \in \mathbb{Z}} c_k(z) e^{2\pi k \theta i},$$

with

$$c_k(z) = \int_0^1 f(\theta, z) e^{-2\pi k \theta i} d\theta.$$

Then we have that $D\mathcal{T}_\omega$ “diagonalizes” with respect to the complex Fourier expansion, in the sense that we have

$$[D\mathcal{T}_\omega(\Psi)f](\theta, z) = [DR_\delta(\psi)c_0](z) + \sum_{k \in \mathbb{Z} \setminus \{0\}} ([L_1(c_k)](z) + [L_2(c_k)](z) e^{2\pi k \omega i}) e^{2\pi k \theta i}, \quad (4)$$

where

$$\begin{aligned} L_1 : \mathcal{B}(W) &\rightarrow \mathcal{B}(W) \\ g(z) &\mapsto \frac{1}{a} \psi' \circ \psi(a z) g(a z), \end{aligned}$$

and

$$\begin{aligned} L_2 : \mathcal{B}(W) &\rightarrow \mathcal{B}(W) \\ g(z) &\mapsto \frac{1}{a} g \circ \psi(a z), \end{aligned}$$

with $\psi = p_0(\Psi)$ and $a = \psi(1)$.

An immediate consequence of this diagonalization is the following.

Proposition 2.1. *Consider*

$$\mathcal{B}_k := \{f \in B \mid f(\theta, x) = u(x) \cos(2\pi k\theta) + v(x) \sin(2\pi k\theta), u, v \in \mathcal{B}(W)\}, \quad (5)$$

then we have that the spaces \mathcal{B}_k are invariant by $D\mathcal{T}_\omega(\Psi)$ for any $k > 0$. Moreover $D\mathcal{T}_\omega(\Psi)$ restricted to \mathcal{B}_k is conjugate to $\mathcal{L}_{k\omega}$ where, for all $\alpha \in \mathbb{R}$, \mathcal{L}_α is defined as a map $\mathcal{L}_\alpha : \mathcal{B}(W) \oplus \mathcal{B}(W) \rightarrow \mathcal{B}(W) \oplus \mathcal{B}(W)$ such that

$$\mathcal{L}_\alpha : \begin{pmatrix} u \\ v \end{pmatrix} \mapsto \begin{pmatrix} L_1(u) \\ L_1(v) \end{pmatrix} + \begin{pmatrix} \cos(2\pi\alpha) & -\sin(2\pi\alpha) \\ \sin(2\pi\alpha) & \cos(2\pi\alpha) \end{pmatrix} \begin{pmatrix} L_2(u) \\ L_2(v) \end{pmatrix}. \quad (6)$$

Proof. Let f be a function in \mathcal{B}_k , then $f(\theta, x) = u(z) \cos(2\pi k\theta) + v(z) \sin(2\pi k\theta)$. Consider the function $c(z) = \frac{u(z) + iv(z)}{2}$. Using formula (4) on the function $u(z) = c(z) + \bar{c}(z)$ and doing some algebra it is easy to see that

$$\begin{aligned} [D\mathcal{T}_\omega(\Psi)](u(z) \cos(2\pi k\theta)) &= [L_1(u)](z) \cos(2\pi k\theta) \\ &\quad + [L_2(u)](z) \cos(2\pi k\omega) \cos(2\pi k\theta) \\ &\quad - [L_2(v)](z) \sin(2\pi k\omega) \sin(2\pi k\theta), \end{aligned}$$

and, doing a similar calculation for $v(z) = i(\overline{c(z)} - c(z))$

$$\begin{aligned} [D\mathcal{T}_\omega(\Psi)](v(z) \sin(2\pi k\theta)) &= [L_1(v)](z) \sin(2\pi k\theta) \\ &\quad + [L_2(u)](z) \sin(2\pi k\omega) \cos(2\pi k\theta) \\ &\quad + [L_2(v)](z) \cos(2\pi k\omega) \sin(2\pi k\theta). \end{aligned}$$

Finally, due to the natural isomorphism between \mathcal{B}_k and $\mathcal{B}(W) \oplus \mathcal{B}(W)$, it is easy to see the conjugacy between $D\mathcal{T}_\omega(\Psi)$ and $\mathcal{L}_{k\omega}$. \square

2.2 Spectrum of \mathcal{L}_ω

In the previous section we have shown that the operator $D\mathcal{T}_\omega(\Psi)$ “diagonalizes” into the infinite sum of operators \mathcal{L}_α with $\alpha = \omega, 2\omega, 3\omega, \dots$ plus the differential of the 1D renormalization operator. Therefore the understanding of \mathcal{L}_α with respect to α is crucial for the understanding of the derivative of the (quasiperiodically extended) renormalization operator. This section is devoted to the study of the spectral properties of \mathcal{L}_ω .

Given a value $\gamma \in \mathbb{T}$, consider the rotation R_γ defined as

$$\begin{aligned} R_\gamma : \mathcal{B}(W) \oplus \mathcal{B}(W) &\rightarrow \mathcal{B}(W) \oplus \mathcal{B}(W) \\ \begin{pmatrix} u \\ v \end{pmatrix} &\mapsto \begin{pmatrix} \cos(2\pi\gamma) & -\sin(2\pi\gamma) \\ \sin(2\pi\gamma) & \cos(2\pi\gamma) \end{pmatrix} \begin{pmatrix} u \\ v \end{pmatrix}. \end{aligned} \quad (7)$$

Then we have the following result.

Proposition 2.2. *For any $\omega, \gamma \in \mathbb{T}$ we have that \mathcal{L}_ω and R_γ commute.*

Proof. It follows from L_1 and L_2 being linear and the fact that any pair of rotations commute. \square

This proposition has the following consequences on the spectrum of \mathcal{L}_ω .

Corollary 2.3. *For any eigenvector (u, v) of \mathcal{L}_ω we have that $R_\gamma(u, v)$ is also an eigenvector of the same eigenvalue for any $\gamma \in \mathbb{T}$.*

Proof. Suppose that (u, v) is an eigenvector of eigenvalue λ , we have $\lambda(u, v) = \mathcal{L}_\omega(u, v)$. Composing in both parts by R_γ and using the last proposition the result follows. \square

Corollary 2.4. *Let λ be a real eigenvalue of \mathcal{L}_ω different from zero and with finite geometric multiplicity. Then, the geometric multiplicity of λ is even.*

Proof. Assume that λ has geometric multiplicity odd. Then its eigenspace is generated by n vectors y_1, y_2, \dots, y_n , with n odd. We can consider $R_\gamma y_i$ for any i , which will also be in the eigenspace of the eigenvalue. Since the vector $R_\gamma y_i$ is linearly independent with y_i but it is in the eigenspace, we have that it is generated by the other eigenvectors. Then one of the original vectors can be replaced by $R_\gamma y_i$. Rearranging the vectors if necessary we can suppose that $y_2 = R_\gamma y_1$. Doing this process repeatedly we will end up with an even number of vectors. \square

On the other hand we have the following result on the dependence of the operator with respect to ω

Proposition 2.5. *The operator \mathcal{L}_ω depends analytically on ω .*

Proof. It follows from the fact that \mathcal{L}_ω is the sum of two bounded linear operators (which do not depend on ω) times an entire function on ω . \square

This result allows us to apply theorems III-6.17 and VII-1.7 of [10]. These results imply that, as long as the eigenvalues of \mathcal{L}_ω do not cross each other, the eigenvalues and their associated eigenspaces depend analytically on the parameter ω .

We want to show that the spectrum of \mathcal{L}_ω is a countable set of eigenvalues with no accumulation points different from zero. In other words, this is the spectrum we would have if \mathcal{L}_ω were a compact operator (Theorem III-6.26 of [10]). In this direction, we show that if we consider \mathcal{L}_ω acting on a space of functions defined on a smaller domain, then it is compact.

Proposition 2.6. *Assume that $W_1 \subset W$ is an open and simply connected set that verifies $\overline{W}_1 \subset W$, $a\overline{W}_1 \subset W_1$ and $\psi(a\overline{W}_1) \subset W_1$, where $\psi = p_0(\Psi)$. Then the operator*

$$\mathcal{L}_\omega : \mathcal{B}(W_1) \oplus \mathcal{B}(W_1) \longrightarrow \mathcal{B}(W_1) \oplus \mathcal{B}(W_1)$$

is compact.

i	λ_i	i	λ_i
1	+7.8412640 +1.5617754 <i>i</i>	13	-0.0637772 +0.0000000 <i>i</i>
2	+7.8412640 -1.5617754 <i>i</i>	14	-0.0637772 -0.0000000 <i>i</i>
3	-2.5029079 +0.0000000 <i>i</i>	15	+0.0430641 +0.0435724 <i>i</i>
4	-2.5029079 +0.0000000 <i>i</i>	16	+0.0430641 -0.0435724 <i>i</i>
5	+0.5114250 +0.1942111 <i>i</i>	17	-0.0178305 +0.0165287 <i>i</i>
6	+0.5114250 -0.1942111 <i>i</i>	18	-0.0178305 -0.0165287 <i>i</i>
7	+0.4881230 +0.4930710 <i>i</i>	19	-0.0101807 +0.0000000 <i>i</i>
8	+0.4881230 -0.4930710 <i>i</i>	20	-0.0101807 -0.0000000 <i>i</i>
9	-0.3995353 +0.0000000 <i>i</i>	21	+0.0075181 +0.0069602 <i>i</i>
10	-0.3995353 +0.0000000 <i>i</i>	22	+0.0075181 -0.0069602 <i>i</i>
11	-0.0982849 +0.0869398 <i>i</i>	23	-0.0029419 +0.0027336 <i>i</i>
12	-0.0982849 -0.0869398 <i>i</i>	24	-0.0029419 -0.0027336 <i>i</i>

Table 1: The first twenty-four eigenvalues of $\mathcal{L}_\omega^{(N)}$, for $\omega = \frac{\sqrt{5}-1}{2}$. For the computation N has been taken equal to 100.

Proof. Since the operators L_1 and L_2 are well defined, it is enough to prove that they are compact.

Let us define the set $K = \overline{W}_1$, which is compact since W is bounded, and the set $B = \{g \in \mathcal{B}(W_1) \mid \exists f \in \mathcal{B}(W) \text{ s. t. } g = f|_K\}$. As B contains all the polynomials with real coefficients, we can use the Mergelyan theorem (see, for instance, [17]) to show that $\overline{B} = \mathcal{B}(W_1)$. Then, it is enough to see that L_1 and L_2 are compact as operators on B (see (11.2.9) in [3]).

Consider U the unit ball of B . To prove that L_i is compact it is enough to prove that $L_i(U)$ is relatively compact (for $i = 1, 2$). To use (9.13.1) in [3] we note that, for each compact set $L \subset W$, there exists a constant m_L such that $|[L_i(f)](z)| \leq m_L$ for all $z \in L$. Taking $L = \overline{W}_1$, (9.13.1) in [3] shows that $L_i(U)$ is relatively compact in $C^0(\overline{W}_1, \mathbb{C})$. To finish the proof, we note that: i) each sequence of elements of $L_i(U)$ has a convergent subsequence to an element of $C^0(\overline{W}_1, \mathbb{C})$; ii) a uniformly convergent sequence of analytic functions on any compact subset of W_1 converges to an analytic function on W_1 . This shows that $L_i(U)$ is relatively compact in B . \square

2.3 Numerical computation of the spectrum of \mathcal{L}_ω

In this section we introduce a discretization of the tangent map S for its numerical study. The discretization described here is the same used in [7], which is a slight modification of the one introduced by Lanford in [12] (see also [13]).

As before, let W be an open set in \mathbb{C} and consider $\mathcal{B}(W)$ the Banach space of real analytic functions, holomorphic on W and continuous on its closure, equipped with the supremum norm.

Let $\mathbb{D}(z_0, \rho)$ be the complex disc centred on z_0 with radius ρ . Given a function $\xi \in$

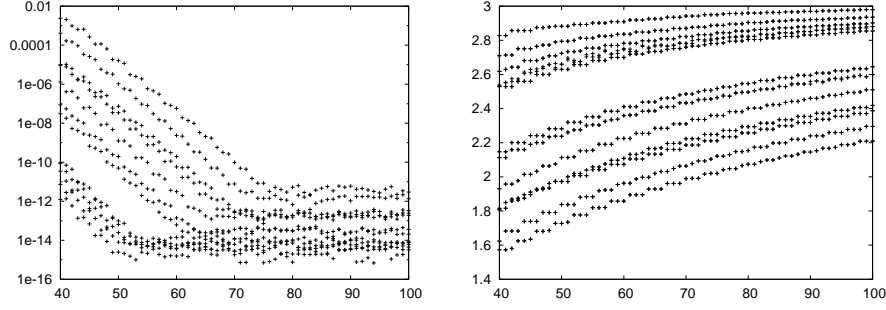


Figure 2: Estimation of the errors and the radii of convergence of the first twenty-four eigenvalues of \mathcal{L}_ω for $\omega = \frac{\sqrt{5}-1}{2}$ with respect to the order of the discretization. See the text for more details.

$\mathcal{B}(\mathbb{D}(z_0, \rho))$, we can consider the following Taylor expansion of ξ around z_0 ,

$$\xi(z) = \sum_{k=0}^{\infty} \xi_k \left(\frac{z - z_0}{\rho} \right)^k. \quad (8)$$

The truncation of this Taylor series at order N induces a projection defined as

$$p_{(N)} : \begin{array}{l} \mathcal{B}(\mathbb{D}(z_0, \rho)) \\ \xi \end{array} \rightarrow \begin{array}{l} \mathbb{R}^{N+1} \\ (\xi_0, \xi_1, \dots, \xi_N). \end{array}$$

On the other hand we have its pseudo-inverse by the left

$$i_{(N)} : \begin{array}{l} \mathbb{R}^{N+1} \\ (\xi_0, \xi_1, \dots, \xi_N) \end{array} \rightarrow \begin{array}{l} \mathcal{B}(\mathbb{D}(z_0, \rho)) \\ \sum_{k=0}^N \xi_k \left(\frac{z - z_0}{\rho} \right)^k; \end{array}$$

in other words $i_{(N)} \circ p_{(N)}$ is the identity on \mathbb{R}^{N+1} . Note also that both maps are linear.

Let W be an open set in \mathbb{C} containing the disc $\mathbb{D}(z_0, \rho)$. Given a map $L : \mathcal{B}(W) \rightarrow \mathcal{B}(W)$, we can approximate its restriction to $\mathcal{B}(\mathbb{D}(z_0, \rho))$ by the discretization $L^{(N)} : \mathbb{R}^{N+1} \rightarrow \mathbb{R}^{N+1}$ defined as $L^{(N)} := p_{(N)} \circ L \circ i_{(N)}$. If the disc $\mathbb{D}(z_0, \rho)$ is strictly contained in W , then it is not difficult to see that $i_{(N)} \circ L^{(N)}(\xi)$ converges to $L(\xi)$ (in the supremum norm) as $N \rightarrow \infty$.

At this point consider the map $\mathcal{L}_\omega : \mathcal{B}(W) \oplus \mathcal{B}(W) \rightarrow \mathcal{B}(W) \oplus \mathcal{B}(W)$ defined by equation (6). If we set $W = \mathbb{D}(z_0, \rho)$ we can use the method described above in each component of $\mathcal{B}(W) \oplus \mathcal{B}(W)$ to discretize \mathcal{L}_ω and approximate it by a map $\mathcal{L}_\omega^{(N)} : \mathbb{R}^{2(N+1)} \rightarrow \mathbb{R}^{2(N+1)}$. Concretely in our computation we have taken $z_0 = \frac{1}{5}$ and $\rho = \frac{3}{2}$.

In Table 1 we have the first twenty-four eigenvalues of $\mathcal{L}_\omega^{(N)}$ for $N = 100$ and $\omega = \frac{\sqrt{5}-1}{2}$. The eigenvalues have been sorted by their modulus, from bigger to smaller. Note that the eigenvalues of the discretized operator are pairs of complex eigenvalues (as anticipated by Corollary 2.3) and accumulate to zero (as anticipated by Proposition 2.6).

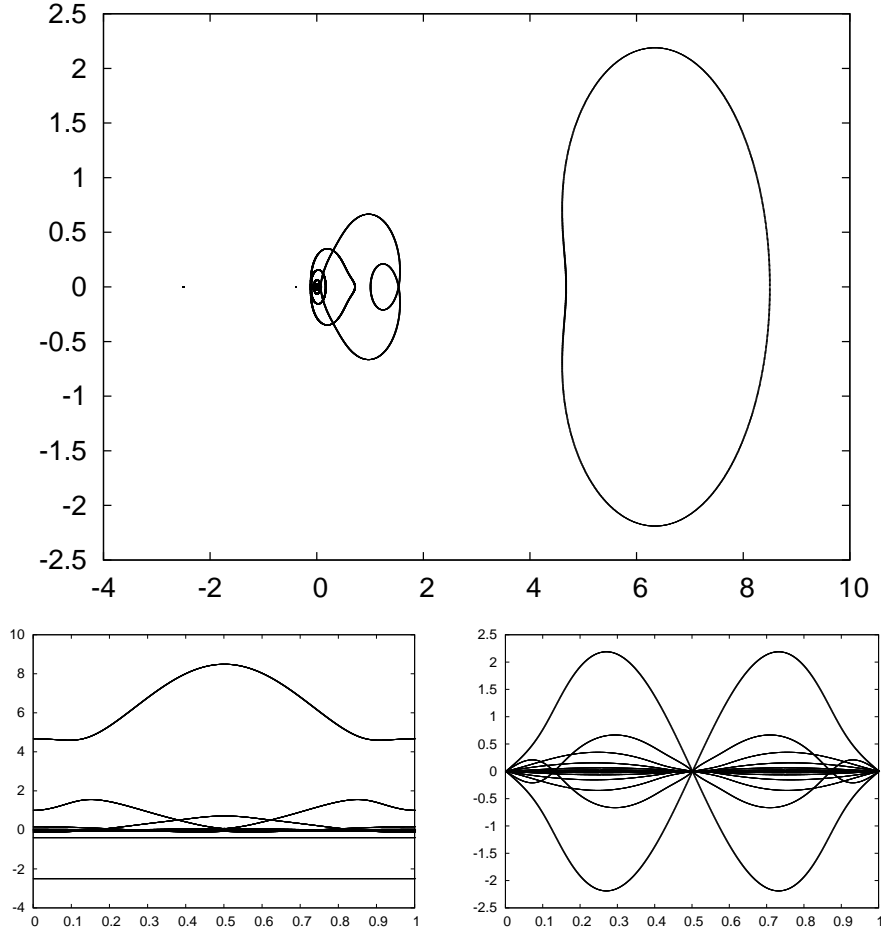


Figure 3: Numerical approximation of the spectrum of \mathcal{L}_ω for $\omega \in \mathbb{T}$. Top: projection in the complex plane of the spectrum when ω varies in \mathbb{T} . Bottom left: evolution of the real part with respect to ω . Bottom right: evolution of the imaginary part with respect to ω .

Given a general linear bounded operator T , we can compute the eigenvalues of a discretization $T^{(N)}$ of the operator in order to study the spectrum of T , but in general the eigenvalues of $T^{(N)}$ might have nothing to do with the spectrum of T . For example an infinite-dimensional operator does not need to have eigenvalues, but a finite-dimensional one will always have the same number of eigenvalues (counted with multiplicity) as the dimension of the space. For this reason we do a couple of numerical test on the results obtained in the discretization of $\mathcal{L}_\omega^{(N)}$.

Consider that we have a real eigenvalue of multiplicity two, or a pair of complex eigenvalues which are persistent for different values of N (the order of the discretization). The first test done to the eigenvalues is to check if the distance between the associated eigenvectors decreases when N is increased. In the left panel of Figure 2 we have the distance between the eigenvectors associated to the same eigenvalue of the operators $\mathcal{L}_\omega^{(N)}$

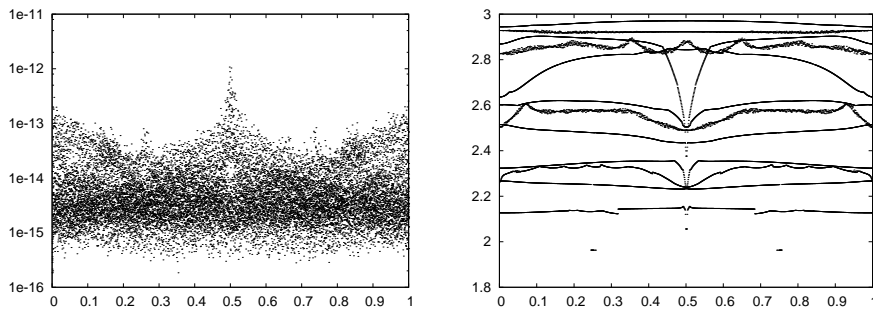


Figure 4: Estimation of the distance between eigenvectors with the same eigenvalue (left) and estimation of the radius of convergence (right) of the first twenty-four eigenvalues of \mathcal{L}_ω with respect to ω . See the text for more details.

and $\mathcal{L}_\omega^{(110)}$ as a graph of N , with N varying from 40 to 100. We have plotted this distance for the first twenty-four eigenvalues. To compute the distance between eigenvectors we have estimated the supremum norm of the difference between the real function represented by each of the vectors, in other words we have computed $\|i^{(N)}(v^{(N)}) - i^{(110)}(v^{(110)})\|_\infty$ in the interval $(z_0 - \rho, z_0 + \rho) = W \cap \mathbb{R}$. Note that the distance seems to go to zero and this suggests that the eigenvectors, namely $v^{(N)}$, converge to a limit v^* . One should expect these eigenvalues to be in the spectrum of \mathcal{L}_ω , but nothing ensures that v^* belongs to the domain of \mathcal{L}_ω .

Let us remark that with the numerical computations done so far, we have only checked that the eigenvectors as elements of $\mathcal{B}(\mathbb{D}(z_0, \rho)) \oplus \mathcal{B}(\mathbb{D}(z_0, \rho))$ converge on the segment $(z_0 - \rho, z_0 + \rho) \subset \mathbb{R}$ but not on the whole set $\mathbb{D}(z_0, \rho)$. We have done a second test to check that the approximate eigenvectors have a domain of analyticity containing $\mathbb{D}(z_0, \rho)$.

Consider that we have a function ξ holomorphic in a domain of the complex plane containing $\mathbb{D}(z_0, \rho)$. If we consider the expansion of ξ given by equation (8), we have that r the radius of convergence of the series around z_0 is given as

$$r = \frac{\rho}{\limsup_{n \rightarrow \infty} (|\xi_n|)^{1/n}}.$$

With the discretization considered here we have an approximation of the terms ξ_n , hence these can be used to compute a numerical estimation of r .

Consider v an eigenvector of the operator \mathcal{L}_ω . We have that $v = (v_1, v_2) \in \mathcal{B}(W) \oplus \mathcal{B}(W)$. Given $v_1^{(N)} = (v_1^{(N)}, v_2^{(N)})$ a numerical approximation of the eigenvector, we can use the procedure described above to estimate the radius of convergence of each v_1 and v_2 . We have done this for the eigenvectors associated to each of the first twenty-four eigenvalues of \mathcal{L}_ω with $\omega = \frac{\sqrt{5}-1}{2}$ (keeping only the smaller of the two radius obtained). The results are displayed on the right panel of Figure 2, where the estimated radius has been plotted with respect to N , the order of the discretization. Note that the estimations give a radius bigger than $\rho = \frac{3}{2}$, which indicates that the eigenvectors are analytic in $\mathbb{D}(z_0, \rho)$, and continuous on its closure, for $z_0 = \frac{1}{5}$ and $\rho = \frac{3}{2}$.

Up to this point, we have considered ω fixed to $\frac{\sqrt{5}-1}{2}$, but the same computations can be done to study the spectrum of \mathcal{L}_ω with respect to the parameter ω . In Figure 3 we display first twenty-four eigenvalues of the map with respect to ω . The set \mathbb{T} has been discretized in a equispaced grid of 1280 points. Recall that the operator \mathcal{L}_ω depends analytically on ω (Proposition 2.5), therefore the spectrum also does (as long as the eigenvalues do not collide, see Theorems III-6.17 and VII-1.7 in [10]).

For this computation we have also made the same test as before to the eigenvalues. The results of these tests are shown in Figure 4. To estimate the convergence of the eigenvectors we have compared the eigenspaces of the eigenvalues of $\mathcal{L}_\omega^{(90)}$ with the eigenspaces associated to $\mathcal{L}_\omega^{(100)}$ for each value of ω in the cited grid of points on \mathbb{T} . The estimation of the radius of convergence has been also done with respect to ω for $N = 90$. We have plotted the estimated error and convergence radius for the first twenty-four eigenvalues in the same figure. Both result indicate that the eigenvalues obtained are reliable.

3 A numerical aided study of the dynamics of the operator

In the one dimensional renormalization theory it is well known that the dynamics around Φ the fixed point of \mathcal{R}_0 plays a major roll in the bifurcations of unimodal 1D maps [2]. For any uniparametric family of 1D maps, the accumulation ratio of consecutive period doubling bifurcations is equal to δ , the dominant eigenvalue of $D\mathcal{R}_0$. By analogy, we believe that a better understanding of the dynamics of R around Φ can help the understanding of the bifurcations in quasiperiodically forced 1D maps [16].

Recall that, in the quasiperiodic version of the renormalization operator that we proposed, instead of a fixed point we have an invariant set $\{(\omega, \Phi)\}$, with $\omega \in \mathbb{T}$. This set includes fixed points and periodic orbits, but these correspond to rational values of ω , which are not of interest.

To study the linearized behaviour around the set $\{(\omega, \Phi)\}$ we could consider S the associated tangent map given by (3) on points of the form (ω, Φ, h) , for some $h \in \mathcal{B}$. We have shown before $D\mathcal{T}_\omega(\Phi)$ leaves the spaces \mathcal{B}_k defined by (5) invariant. Moreover, the operator restricted to these spaces is conjugated to $\mathcal{L}_{k\omega}$, which has its dominant eigenvalue outside the unit circle for any ω . Therefore, one can expect the map S to have a expanding behaviour on the third component. Nevertheless, we might investigate numerically if there exists a dominant invariant direction of expansiveness and its shape. With this aim we consider the map A defined as:

$$\begin{aligned}
 A: \mathbb{T} \times \mathcal{B}_1 &\rightarrow \mathbb{T} \times \mathcal{B}_1 \\
 (\omega, v) &\mapsto \left(2\omega, \frac{\mathcal{L}_\omega v}{\|\mathcal{L}_\omega v\|} \right).
 \end{aligned} \tag{9}$$

We can use the discretization of \mathcal{L}_ω described in Section 2.3 to study numerically the map A . As \mathcal{B}_1 can be identified with the space $\mathcal{B}(W) \oplus \mathcal{B}(W)$, we consider the coordinates

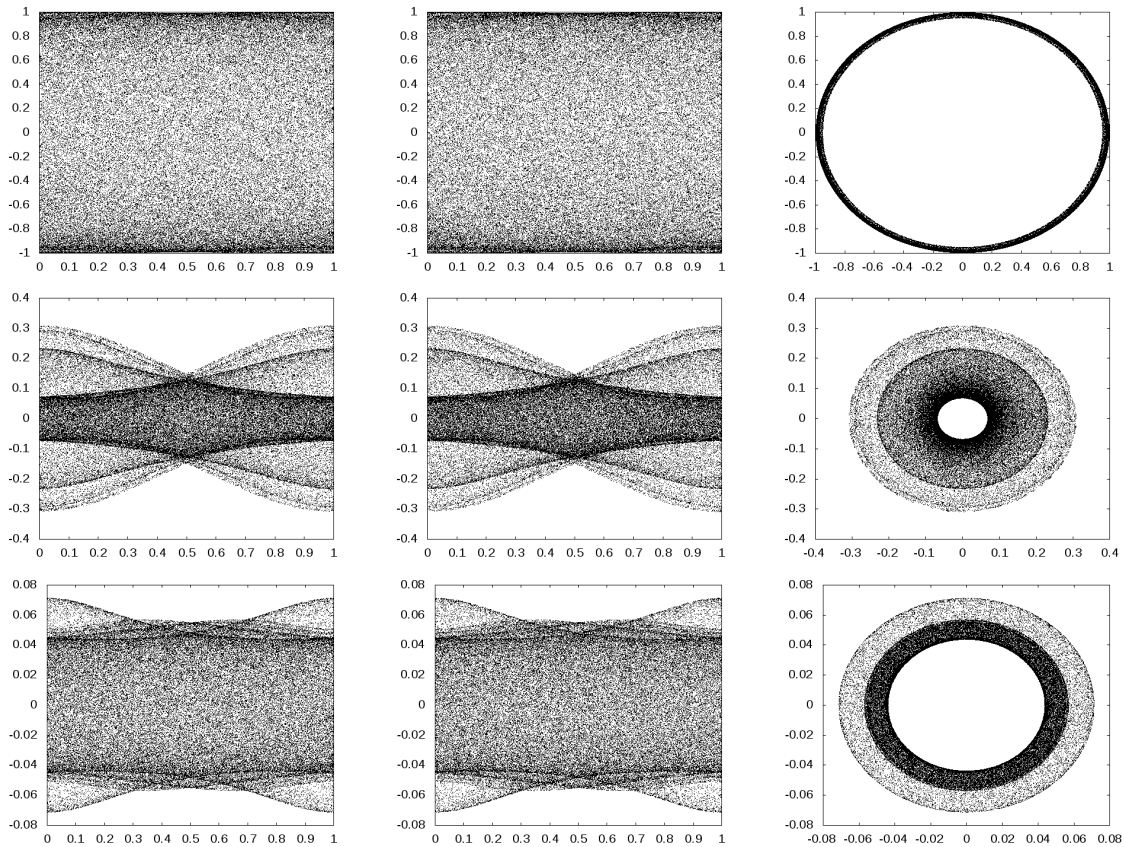


Figure 5: Planar projections of the attractor of the map (9). From left to right, and top to bottom we show (ω, x_0) , (ω, y_0) , (x_0, y_0) , (ω, x_2) , (ω, y_2) , (x_2, y_2) , (ω, x_4) , (ω, y_4) and (x_4, y_4) .

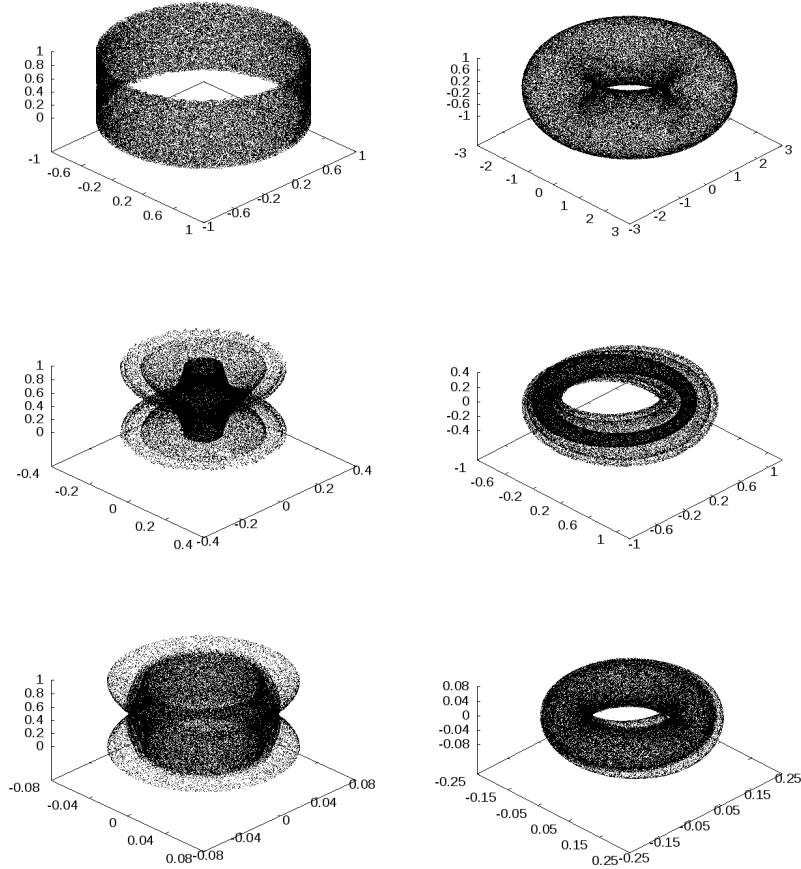


Figure 6: Several spatial projections of the attractor of the map (9). In the left hand side of the picture we have a plot (from top to bottom) of the projections in the coordinates (ω, x_0, y_0) , (ω, x_2, y_2) and (ω, x_4, y_4) . The right hand side shows the image of the left side projections taking a map that embeds the solid torus in \mathbb{R}^3 (see the text for more details).

of $v = (x, y)$ given by this splitting. Following the discretization, each function $x \in \mathcal{B}(W)$ is approximated by a vector $(x_0, x_1, x_2, \dots, x_N) \in \mathbb{R}^{N+1}$ where x_i is the i -th coefficient of the Taylor expansion for x around 0. This also holds for y , the second component of v . Therefore, each element v in \mathcal{B}_1 can be approximated by a vector $(x_0, x_1, \dots, x_N, y_0, \dots, y_N)$ in $\mathbb{R}^{2(N+1)}$. We can use this discretization to study the dynamics of A . Let $A^{(N)}$ denote this approximation, and we call N the order of the discretization.

Given an initial point $v_0 = (x^0, y^0) \neq 0$, we have iterated this point by the map for a certain transient N_1 and then we have plotted the following N_2 iterates. Figures 5 and 6 show different projections of the resulting attracting set. The values taken to elaborate this particular set of figures are $N = 30$, $N_1 = 2000$ and $N_2 = 80000$. We display the coordinates corresponding to the first even Taylor coefficients of the functions x and y . The odd Taylor coefficients obtained were all equal to zero, so we have omitted them. This last observation suggests that the attractor is contained in the set of even functions (note that the subspace of \mathcal{B}_1 consisting of all the even functions is invariant by \mathcal{L}_ω).

The same computations have been done for bigger values of N leading to the same results. This indicates that the set obtained is stable with respect to the order of discretization, therefore it can be expected to be close to the true attracting set of the original system.

Let us remark that we have not made explicit the initial values of w_0 and v_0 taken for the computations. Indeed, the results seem to be independent of these values. We have repeated this computation taking as initial value of v_0 all the elements of the canonical base of the discretized space $\mathbb{R}^{2(N+1)}$ and we have always obtained the same results. We have also repeated the computations for several irrational values of ω_0 obtaining always the same results.

The numerical approximation of the attractor displayed in Figure 5 and Figure 6 reveal the rotational symmetry of the attractor.

3.1 Rotational symmetry elimination and the dyadic solenoid

Given $\gamma \in \mathbb{T}$, consider the following auxiliary function

$$\begin{aligned} t_\gamma : \mathcal{B} &\rightarrow \mathcal{B} \\ v(\theta, z) &\mapsto v(\theta + \gamma, z). \end{aligned}$$

Given a one dimensional map, the effects caused by a quasiperiodic perturbation h and by $t_\gamma(h)$ should be essentially the same. This is what causes the rotational symmetry in the attracting set of A .

Let \mathcal{B}_1 be the subspace of \mathcal{B} defined by (5) for $k = 1$. Note that t_γ restricted to \mathcal{B}_1 corresponds indeed to R_γ given by (7), which commutes with \mathcal{L}_ω .

Given $\theta_0 \in \mathbb{T}$ and $z_0 \in W \cap \mathbb{R}$, consider the sets

$$\mathcal{B}'_1 = \mathcal{B}'_1(\theta_0, z_0) = \{f \in \mathcal{B}_1 \mid f(\theta_0, z_0) = 0, \partial_\theta f(\theta_0, z_0) > 0\}.$$

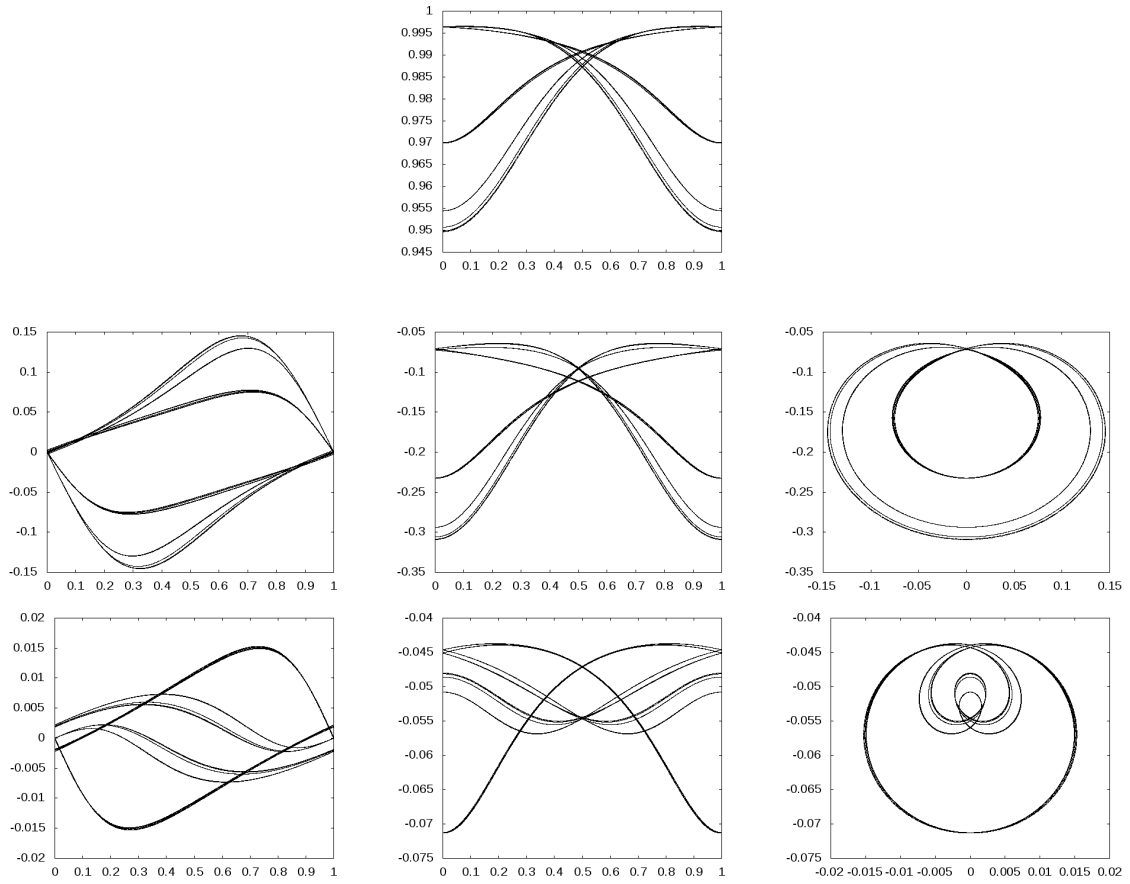


Figure 7: Several planar projections of the section of attractor of the map (10). From left to right, and top to bottom we have the projections in the coordinates (ω, y_0) , (ω, x_2) , (ω, y_2) , (x_2, y_2) , (ω, x_4) , (ω, y_4) and (x_4, y_4) .

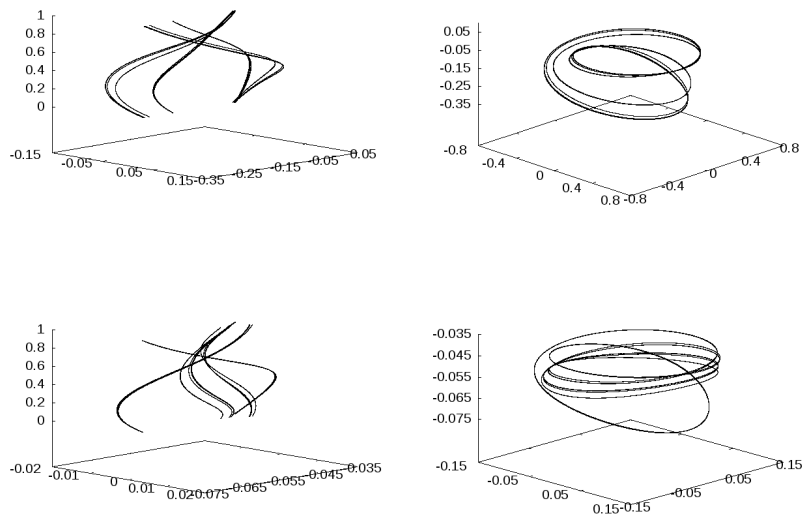


Figure 8: Several spatial projections of the intersection of the attractor of the map (10). Left figures correspond to the projection to the coordinates (ω, x_2, y_2) (top) and (ω, x_4, y_4) (bottom). In the right hand side there are displayed the image of the left side projections taking a map that embeds the solid torus in \mathbb{R}^3 (see the text for more details).

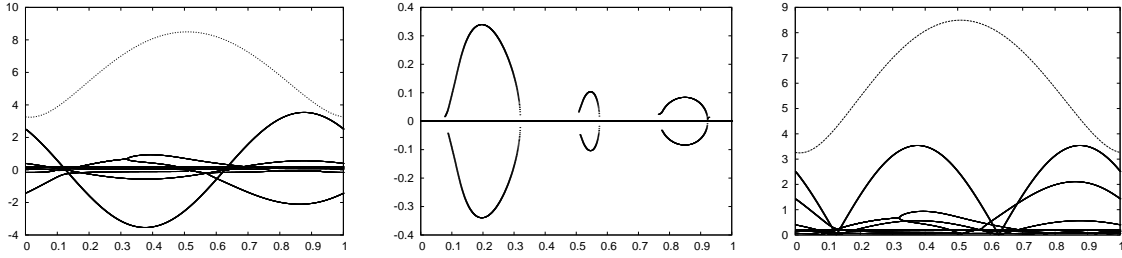


Figure 9: Numerical approximation of the spectrum of \mathcal{L}'_ω with respect to the parameter ω . From left to right we have the real part, the imaginary part and the modulus of the first eight eigenvalues of \mathcal{L}'_ω with respect to ω .

Recall that any function $v \in \mathcal{B}_1$ can be written as $v(\theta, z) = x(z) \cos(2\pi\theta) + y(z) \sin(2\pi\theta)$, with $x, y \in \mathcal{B}(W)$. For any v such that $x(z_0)y(z_0) \neq 0$, we have that $v(\theta_0 + \gamma, z_0) = 0$ for the values $\gamma = \arctan(-x(z_0)/y(z_0))/2\pi - \theta_0$ and $\gamma = \arctan(-x(z_0)/y(z_0))/2\pi - \theta_0 + 1/2$, but only one of these two values satisfies $\partial_\theta v(\theta_0 + \gamma, x_0) > 0$. Therefore, for any $v \in \mathcal{B}_1 \setminus \{v \mid v(\theta, z_0) = 0, \forall \theta \in \mathbb{T}\}$ there exists a unique $\gamma_0 \in \mathbb{T}$ such that $t_{\gamma_0}(v) \in \mathcal{B}'_1(\theta_0, z_0)$.

The following map eliminates the rotational symmetry by projecting the points in \mathcal{B}_1 into the set \mathcal{B}'_1 .

$$\begin{aligned}
 B : \mathbb{T} \times \mathcal{B}'_1 &\rightarrow \mathbb{T} \times \mathcal{B}'_1 \\
 (\omega, v) &\mapsto \left(2\omega, \frac{\mathcal{L}'_\omega v}{\|\mathcal{L}'_\omega v\|} \right),
 \end{aligned} \tag{10}$$

with

$$\begin{aligned}
 \mathcal{L}'_\omega : \mathcal{B}'_1 &\rightarrow \mathcal{B}'_1 \\
 v &\mapsto t_{\gamma(v)}(\mathcal{L}_\omega(v)),
 \end{aligned}$$

where $\gamma(v)$ is chosen such that $t_{\gamma(v)}(\mathcal{L}_\omega(v)) \in \mathcal{B}'_1$.

We can use again the discretization described in Section 2.3 to approximate numerically the dynamics of B as we have done with A . For the numerical simulation of the operator, we have taken $\theta_0 = 0$ and $x_0 = 0$. After discretization, the set $\mathcal{B}'_1(0, 0)$ is identified in $\mathbb{R}^{2(N+1)}$ with the half hyperplane

$$\{(x, y) \in \mathbb{R}^{2(N+1)} \mid x_0 = 0 \text{ and } y_0 > 0\},$$

where x_0 and y_0 are respectively the first components of x and y .

In Figure 7 and Figure 8 we display different projections of the attracting set obtained iterating the map B .

Note that the different projections of the attracting set displayed in Figure 7 keep a big resemblance with the plots of the dyadic solenoid displayed in Figure 5 of [14]. Indeed we believe that the attractor is the inclusion of a dyadic solenoid in \mathcal{B}'_1 . For more details on the definition and the dynamics of the solenoid map see [1, 11, 14, 18].

In Figure 9 we display a numerical approximation of the operator \mathcal{L}'_ω defined above. We can observe that for every value of ω there exists a single dominant eigenvalue. We believe

that this dyadic solenoid similarity is explained by the fact that the second component of (10) contracts all point towards the dominant eigenspace (which depends on ω) while the first component is expansive in ω . This is essentially the same mechanism that creates the dyadic solenoid in \mathbb{R}^3 .

References

- [1] H. Broer and F. Takens, *Dynamical systems and chaos*, vol. 172 of Applied Mathematical Sciences, Springer, New York, 2011.
- [2] W. de Melo and S. van Strien, *One-dimensional dynamics*, vol. 25 of Ergebnisse der Mathematik und ihrer Grenzgebiete (3) [Results in Mathematics and Related Areas (3)], Springer-Verlag, Berlin, 1993.
- [3] J. Dieudonné, *Foundations of modern analysis*, Academic Press, New York, 1969, Enlarged and corrected printing, Pure and Applied Mathematics, Vol. 10-I.
- [4] R. Fabbri, T. Jäger, R. Johnson and G. Keller, A Sharkovskii-type theorem for minimally forced interval maps, *Topol. Methods Nonlinear Anal.*, **26** (2005), 163–188.
- [5] U. Feudel, S. Kuznetsov and A. Pikovsky, *Strange nonchaotic attractors*, vol. 56 of World Scientific Series on Nonlinear Science. Series A: Monographs and Treatises, World Scientific Publishing Co. Pte. Ltd., Hackensack, NJ, 2006.
- [6] À. Jorba, C. Núñez, R. Obaya and J. Tatjer, Old and new results on strange nonchaotic attractors, *Internat. J. Bifur. Chaos Appl. Sci. Engrg.*, **17** (2007), 3895–3928.
- [7] À. Jorba, P. Rabassa and J. C. Tatjer, A renormalization operator for 1D maps under quasi-periodic perturbations, *Nonlinearity*, **28** (2015), 1017–1042.
- [8] À. Jorba, P. Rabassa and J. Tatjer, Period doubling and reducibility in the quasi-periodically forced logistic map, *Discrete Contin. Dyn. Syst. Ser. B*, **17** (2012), 1507–1535.
- [9] À. Jorba and J. Tatjer, A mechanism for the fractalization of invariant curves in quasi-periodically forced 1-D maps, *Discrete Contin. Dyn. Syst. Ser. B*, **10** (2008), 537–567.
- [10] T. Kato, *Perturbation theory for linear operators*, Die Grundlehren der mathematischen Wissenschaften, Band 132, Springer-Verlag New York, Inc., New York, 1966.

- [11] A. Katok and B. Hasselblatt, *Introduction to the modern theory of dynamical systems*, vol. 54 of Encyclopedia of Mathematics and its Applications, Cambridge University Press, Cambridge, 1995.
- [12] O. Lanford III, A computer-assisted proof of the Feigenbaum conjectures, *Bull. Amer. Math. Soc. (N.S.)*, **6** (1982), 427–434.
- [13] O. Lanford III, Computer assisted proofs, in *Computational methods in field theory (Schladming, 1992)*, vol. 409 of Lecture Notes in Phys., Springer, Berlin, 1992, 43–58.
- [14] J. Milnor, On the concept of attractor, *Comm. Math. Phys.*, **99** (1985), 177–195.
- [15] A. Prasad, S. Negi and R. Ramaswamy, Strange nonchaotic attractors, *Internat. J. Bifur. Chaos Appl. Sci. Engrg.*, **11** (2001), 291–309.
- [16] P. Rabassa, À. Jorba and J. Tatjer, A numerical study of universality and self-similarity in some families of forced logistic maps, *Internat. J. Bifur. Chaos Appl. Sci. Engrg.*, **23** (2013), 1350072, 11.
- [17] W. Rudin, *Real and complex analysis*, 3rd edition, McGraw-Hill Book Co., New York, 1987.
- [18] S. Smale, Differentiable dynamical systems, *Bull. Amer. Math. Soc.*, **73** (1967), 747–817.